Published in final edited form as:
Dev Biol. 2007 October 1; 310(1): 154–168.

Hand transcription factors cooperatively regulate development of the distal midline mesenchyme

Ana C. Barbosa[1], **Noriko Funato**[1], **Shelby Chapman**[1], **Marc D. McKee**[2], **James A. Richardson**[1,3], **Eric N. Olson**[1†], and **Hiromi Yanagisawa**[1†]

1*Department of Molecular Biology, University of Texas Southwestern Medical Center, Dallas, TX 75390-9148, U.S.A.*

2*Faculty of Dentistry and Department of Anatomy and Cell Biology, McGill University, Montreal, Quebec, Canada*

3*Department of Pathology, University of Texas Southwestern Medical Center, Dallas, TX 75390-9148, U.S.A.*

Abstract

Hand proteins are evolutionally conserved basic helix-loop-helix (bHLH) transcription factors implicated in development of neural crest-derived tissues, heart and limb. *Hand1* is expressed in the distal (ventral) zone of the branchial arches, whereas the *Hand2* expression domain extends ventrolaterally to occupy two-thirds of the mandibular arch. To circumvent the early embryonic lethality of *Hand1* or *Hand2*-null embryos and to examine their roles in neural crest development, we generated mice with neural crest-specific deletion of *Hand1* and various combinations of mutant alleles of *Hand2*. Ablation of *Hand1* alone in neural crest cells did not affect embryonic development, however, further removing one *Hand2* allele or deleting the ventrolateral branchial arch expression of *Hand2* lead to a novel phenotype presumably due to impaired growth of the distal midline mesenchyme. Although we failed to detect changes in proliferation or apoptosis between the distal mandibular arch of wild-type and *Hand1/Hand2* compound mutants at embryonic day (E)10.5, dysregulation of *Pax9*, *Msx2* and *Prx2* was observed in the distal mesenchyme at E12.5. In addition, the inter-dental mesenchyme and distal symphysis of Meckel's cartilage became hypoplastic, resulting in the formation of a single fused lower incisor within the hypoplastic fused mandible. These findings demonstrate the importance of Hand transcription factors in the transcriptional circuitry of craniofacial and tooth development.

Introduction

Defects in migration, expansion, and differentiation of neural crest cells result in a variety of birth defects affecting craniofacial and cardiovascular structures. The neural crest is a transient and pluripotent population of cells that is formed in the dorsal lip of the neural tube as a result of inductive interactions between the neural plate and the surface ectoderm (Selleck MA et al., 1999). During craniofacial development, neural crest cells migrate ventrolaterally and populate the branchial arches, where they proliferate and form the frontonasal process and discrete

†Corresponding authors: Hiromi Yanagisawa, M.D., Ph.D., Department of Molecular Biology, University of Texas Southwestern Medical Center, 5323 Harry Hines Blvd., Dallas, TX 75390-9148, Ph: 214-648-7723, Fx: 214-648-1488, e-mail: hiromi.yanagisawa@utsouthwestern.edu or Eric N. Olson, Ph.D., Department of Molecular Biology, University of Texas Southwestern Medical Center, 5323 Harry Hines Blvd., Dallas, TX 75390-9148, Ph: 214-648-1627, Fx: 214-648-1196, e-mail: eric.olson@utsouthwestern.edu.

swellings that demarcate each branchial arch. Lineage trace studies utilizing a *Wnt1-Cre* transgene and the ROSA26 conditional reporter (R26R) mouse line have confirmed *in vivo* that cranial neural crest cells eventually differentiate into bone, cartilage, teeth, cranial ganglia, and connective tissue of the face and neck (Chai et al., 2000; Chai and Maxson, 2006).

Early in embryonic development, the ectomesenchyme of the mandibular arch can be divided along a horizontal axis into two equal parts that have distinct developmental capabilities. The rostral (oral) ectomesenchyme participates in tooth formation via interactions with the overlying oral ectoderm, while the caudal (aboral) mandibular ectomesenchyme gives rise to Meckel's cartilage (reviewed in Miletich and Sharpe, 2004). Meckel's cartilage is unique among cartilages in that it exists provisionally prior to permanent mandibular bone formation in the first branchial arch (Sohal et al., 1999).

The mandible first appears as a mesenchymal condensation at E11.5 in mice. At around E13.5, bone begins to form by means of intramembranous ossification, which involves differentiation of mesenchymal precursors to active osteoblasts along the Meckel's cartilage in a proximo-distal direction (Ramaesh and Bard, 2003). As intramembranous ossification proceeds, BrdU-positive proliferating cells diminish from the body of the mandible except at the proximal and distal symphysis of Meckel's cartilage where proliferating cells contribute to the lengthening mandible (Ramaesh and Bard, 2003). By E16.5, the body of the mandibular bone is surrounded by a periosteum and the distal region of the mandible encloses the Meckel's cartilage followed by gradual disintegration of Meckel's cartilage (Ramaesh and Bard, 2003). In contrast to the posterior (proximal) end of Meckel's cartilage, which undergoes endochondral ossification to form middle ear ossicles (Kronenberg, 2003), the anterior (distal) and intermediate portions of Meckel's cartilage degenerate, undergo apoptosis, and are resorbed and replaced by bone (Ishizeki et al., 1999; Trichilis and Wroblewski, 1997). Recently, it was reported that the development and growth of incisors may contribute to osteoclast differentiation and activation, as well as initiation of resorption of Meckel's cartilage (Sakakura et al., 2005).

Tooth development is regulated by inductive tissue interactions between the oral epithelium and the subjacent mesenchyme of the first branchial arch. Numerous signaling pathways have been implicated in each stage of tooth development (reviewed in Matalova et al., 2004). In particular, Fibroblast growth factor-8 (Fgf8), bone morphogenetic protein-4 (Bmp4), sonic hedgehog (Shh), and Wnt7b are epithelial-derived growth factors that induce an auto-regulatory positive feedback loop as well as mutual inhibitory signals to form incisor-molar boundaries within the epithelium (Hardcastle et al., 1998; Jeong et al., 2004; Sasaki et al., 2005; Stottmann et al., 2001). Tooth initiation becomes morphologically distinguishable between embryonic day (E) 11.5 and E12 when the oral ectoderm thickens in prospective tooth-forming regions of the mandibular and maxillary arches (reviewed in Tucker and Sharpe, 2004). This thickened ectoderm, known as the dental lamina, proliferates and starts to invaginate into the underlying neural crest-derived mesenchyme. Around E13.5 at the bud stage of tooth development, the mesenchyme proliferates and condenses around the developing epithelial bud. During this period, the mesenchyme induces the epithelial enamel knot, which becomes the signaling center of the developing tooth. By E14.5, the tooth bud takes the shape of a cap, and neural crest-derived ectomesenchymal cells are concentrated at the dental papilla. Cytodifferentiation of the tooth occurs after E16.5 at the bell stage, in which the ectoderm gives rise to the enamel- secreting ameloblasts, and the ectomesenchyme to dentine-secreting odontoblasts, pulp, and alveolar bone.

In the present work, we investigated the function of *Hand* genes in the development of mandibular arch derivatives. The class II bHLH proteins Hand1 (eHand, Thing1, and Hxt) and Hand2 (dHand, Thing2, and Hed) are expressed in partially overlapping domains in postmigratory neural crest cells in the branchial arches. *Hand1* expression is confined to the

ventral one-third of the mandibular arch and arch two, whereas *Hand2* is expressed in the ventral two-thirds of the mandibular arch and arch two (Clouthier et al., 2000; Cserjesi et al., 1995; Srivastava et al., 1995; Srivastava et al., 1997). *Hand1*$^{-/-}$ embryos die by E8.5 due to yolk sac deficiency and *Hand2*$^{-/-}$ embryos die around E10.5 because of cardiac insufficiency (Firulli et al., 1998; Srivastava et al., 1997). Although *Hand2*$^{-/-}$ embryos show retarded branchial arch development and increased apoptosis, it is not clear whether the phenotype is a primary effect of the absence of *Hand2* or secondary to heart abnormalities.

Despite early embryonic lethality of homozygous embryos, other genetically manipulated mice offer some insights into the role of *Hand* genes in the development of branchial arch-derived tissues. Mice lacking the endothelin-1-dependent *Hand2* branchial arch enhancer die perinatally and exhibit a spectrum of craniofacial defects, including cleft palate, mandibular hypoplasia and cartilage malformations (Yanagisawa et al., 2003). Lineage analysis using *Hand2*-Cre:R26R embryos showed *Hand2*-progeny cells in both mandibular and molar mesenchyme at around E11.5, and later in dental papilla as well as in chondrogenic and osteogenic structures including Meckel's cartilage (Ruest et al., 2003). In transgenic embryos expressing β-galactosidase under the same 7.4kb upstream region of the *Hand2* gene, transgene expression was observed in the broad mesenchyme of the incisor region. It was also reported that treatments of tooth germ explants with *Hand2* anti-sense oligodeoxynucleotide resulted in impaired differentiation of ameloblasts and odontoblasts, suggesting a potential role of Hand2 in early tooth formation (Abe et al., 2002).

To further explore roles of *Hand* genes during craniofacial development, we deleted the *Hand1* gene in the branchial arch ectomesenchyme using *Cre* recombinase controlled by the neural crest cell-specific *Wnt1* promoter. We also manipulated the expression domain and the level of both *Hand* genes in the branchial arches during embryogenesis by generating compound mutants carrying *Hand1* conditional alleles and mutated *Hand2* alleles. We found that development of the distal midline mesenchyme of the mandibular arch was sensitive to the total *Hand* gene dosage.

MATERIALS AND METHODS

Mouse strains

Hand1-null allele, referred to as *Hand1*^{lacZ} or *Hand1*^{KO}, and *Hand*1 conditional allele, referred to as *Hand1*^{loxP}, have been described previously (Firulli et al., 1998; McFadden et al., 2005). *Hand2*-null allele and *Hand2* mutant allele lacking the ventrolateral branchial arch enhancer, referred to as *Hand2*^{BA}, have been described elsewhere (Srivastava et al., 1997; Yanagisawa et al., 2003). A transgenic mouse line expressing Cre recombinase under the neural crest specific promoter *Wnt1* (*Wnt1::Cre*) has been previously characterized (Jiang et al., 2000). Animals were kept on a 12h/12h light/dark cycle under specific, pathogen-free conditions. Wild-type or heterozygous littermates were used as controls. All animal experimental procedures were reviewed and approved by the Institutional Animal Care and Use Committees.

RT-PCR

Mandibular and second branchial arches were collected from wild-type (*Hand1*$^{loxP/loxP}$; n=13), mutant (*Wnt1::Cre*; *Hand1*$^{lacZ/loxP}$; n=9, *Wnt1::Cre*;*Hand1*$^{loxP/loxP}$; n=8) and heterozygous (*Hand1*$^{lacZ/loxP}$; n=14) embryos at E10.5 and pooled for RNA preparation. Total RNA was isolated using Trizol (Invitrogen) according to the manufacturer's protocol. Randam hexamer-primed first-strand cDNAs were synthesized from 1 μg of total RNA using Superscript II (Invitrogen). Real-time PCR was performed using Assayson-Demand TaqMan primers and probes for mouse *Hand1* and *Hand2* (Applied Biosystems) on an ABI PRISM 7000 sequence detection system (Applied Biosystems). Expression levels were normalized to 18S RNA.

Cartilage and bone staining

Euthanized newborn mice were skinned, eviscerated and fixed in 95% ethanol and stained with Alizarin Red and Alcian Blue to examine bone and cartilage formation, respectively (Yanagisawa et al., 1998). Cartilaginous fetal skeletons (E15.5) were prepared and stained with Alcian Blue as previously described (Jegalian and De Robertis, 1992).

β-galactosidase staining

Embryos were harvested and rinsed with PBS and pre-fixed in PBS containing 2% paraformaldehyde and 0.25% glutaraldehyde for 1–3 hours on ice. Staining for β-gal activity was performed as previously described (McFadden et al., 2000).

Histology

P1 pups were euthanized and heads were harvested and fixed in 10% phosphate-buffered formalin at 4°C. Embryos were harvested and fixed overnight in 4% paraformaldehyde. Paraffin-embedded sections were prepared and stained with hematoxylin and eosin for general histology. β-galactosidase-stained sections were counter-stained with nuclear fast red. Von Kossa staining was used to detect mineralization. Heads from P1 pups were also embedded in LR White acrylic resin, and mineralized bone and tooth tissues were visualized in semi-thin, 1 μm-thick sections by von Kossa staining followed by counterstaining with toluidine blue.

Section *in situ* hybridization

E10.5 and E14.5 embryos were harvested and fixed in 4% paraformaldehyde overnight at 4° C. Riboprobes for *Hand1* and *Hand2* (McFadden et al., 2005), *Fgf8* (Meyers and Martin, 1999), *Shh* (Echelard et al., 1993), *BMP4* (Jones et al., 1991), *Wnt7b* (Parr et al., 1993), *Collagen α1(II)* (Ducy et al., 1997); *Osteocalcin* (Ducy and Karsenty, 1995); Indian hedgehog and *Collagen α1(X)* (Akiyama et al., 1999) and *Collagen α1(I)* (Aigner et al., 1995) were prepared with ^{35}S-UTP (Amersham) using the Maxiscript In Vitro Transcription Kit (Ambion). *In situ* hybridization was performed as described (Shelton et al., 2000).

Whole mount *in situ* hybridization

Embryos were harvested at E12.5 and fixed in 4% paraformaldehyde overnight at 4°C. Whole mount *in situ* hybridization was performed using digoxigenin-labeled riboprobes for *Hand1* and *Hand2* (Clouthier et al., 2000), *Shh* (Echelard et al., 1993), *Pax9* (Neubuser et al., 1995), *Patched* (Goodrich et al., 1996), *Prx1/MHox* (Cserjesi et al., 1992), *Prx2/S8* (Opstelten et al., 1991), *Msx1* and *Msx2* (Thomas et al., 1998) as previously described (Riddle et al., 1993).

TUNEL and immunohistochemistry

Embryos were harvested at E10.5 and E14.5 then fixed overnight in 4% paraformaldehyde and embedded in paraffin. Free DNA ends were detected on transverse sections of embryos using the In situ cell death detection kit (Roche) according to the manufacturer's protocol. Immunohistochemical detection of phosphorylated Histone H3 was performed as previously described (Shin et al., 2002).

Micro-computed tomography

Mandibular scans were performed on a standard desktop micro-computed tomography (micro-CT) instrument from Skyscan (Model 1072; AartsePaar, Belgium). This instrument has an 80-KeV sealed, air-cooled, microfocused X-ray source with a polychromatic beam derived from a tungsten target and with a spot size of less than 8 um. For these analyses, the X-ray source was operated at maximum power (80 KeV) and at 100 uA. Images were captured using a 12-bit, cooled CCD camera (1024 × 1024 pixels) coupled by a fiber optics taper to the scintillator.

Prior to micro-CT analysis, mandibles with their dentition were chemically fixed overnight in 4% paraformaldehyde and 1% glutaraldehyde in 0.1M sodium cacodylate buffer, and then transferred to buffer alone. Mandibles with their dentition were wrapped in thin-film plastic wrap to prevent dessication, and scanned by micro-CT during rotation of the samples for approximately 30 minutes. Cross-sectional x-ray slices were reconstructed using the Skyscan tomography software based on triangular surface rendering to give a three-dimensional distribution of the calcified tissue and soft tissue.

Results

Deletion of *Hand1* in neural crest cells

To delete *Hand1* specifically in neural crest cells, we crossed *Hand1*$^{loxP/loxP}$ females to *Wnt1::Cre*; *Hand1*$^{lacZ/+}$ heterozygous males. The *Wnt1* promoter-driven *Cre* is expressed in pre-migratory neural crest cells and deletes efficiently in neural crest cells *in vivo* (Chai et al., 2000; Jiang et al., 2000). To confirm that the *Hand1*^{loxP} allele was efficiently recombined *in vivo*, we analyzed *Hand1* expression in E10.5 *Wnt1::Cre; Hand1*$^{loxP/lacZ}$ (hereafter referred to as *Hand1*$^{NCKO/KO}$) embryos by *in situ* hybridization. In wild-type embryos, *Hand1* was expressed in the distal (ventral) portion of the mandibular branchial arch (Fig. 1A, panel a, arrow) and *Hand2* was expressed from the distal (ventral) to the ventrolateral portion of the mandibular branchial arch (Fig.1A, panel c). Consistent with a previous report, the *Hand1* expression domain was completely included within the *Hand2* domain (Clouthier et al., 2000). In contrast, *Hand1* expression was absent in the mandibular arch of *Hand1*$^{NCKO/}$KO embryos (Fig. 1A, panel b, arrow). The absence of *Hand1* did not affect *Hand2* expression (Fig. 1A, panel d). As expected, *Hand1* expression was unaffected in the heart and limb of *Hand1*$^{NCKO/KO}$ mice (data not shown).

To quantitate *Hand1* expression in *Hand1*$^{NCKO/KO}$ neural crest cells, real time RT-PCR was performed using RNA extracted from mandibular and second branchial arches of E10.5 embryos. As Fig. 1B shows, *Hand1* expression was almost undetectable in the *Hand1*$^{NCKO/KO}$ branchial arches (both in Wnt1::Cre; *Hand1*$^{loxP/loxP}$ and Wnt1::Cre; *Hand1*$^{loxP/lacZ}$), while the *Hand2* level was comparable among the genotypes, indicating that *Hand2* was not upregulated to compensate for the loss of *Hand1*. These data indicate that *Hand1* was efficiently deleted in the branchial arches of *Hand1*$^{NCKO/KO}$ embryos.

Next, we examined *Hand1*$^{NCKO/KO}$ pups at both postnatal day (P)1 and P28 for defects in craniofacial structures by gross morphology. Unexpectedly, *Hand1*$^{NCKO/KO}$ pups were anatomically normal and were fertile, and no embryonic lethality was observed (data not shown). These findings suggest that the overlapping expression of *Hand2* in the distal region of the rostral mandibular arch can compensate for the loss of *Hand1*.

Manipulation of *Hand* genes in the branchial arches during development

To test the possibility that *Hand2* compensates for functions of *Hand1* during branchial arch development, we manipulated expression levels and domains of *Hand2* during embryonic development. We generated *Hand1*$^{NCKO/KO}$ mice that were heterozygous for the *Hand2*-null allele (*Hand2*$^{KO/+}$), or homozygous for a *Hand2*-mutant allele lacking the branchial arch enhancer (*Hand2*$^{BA/BA}$), to reduce the *Hand2* dosage in the branchial arches. *Hand2*$^{BA/BA}$ mice were previously shown to develop a hypoplastic mandible, deformed tympanic ring and cleft palate (Yanagisawa et al., 2003) attributable to the loss of *Hand2* expression specifically in the ventrolateral domain of the mandibular arch. Therefore, *Hand1*$^{NCKO/KO}$; *Hand2*$^{BA/BA}$ mice lack the ventrolateral expression of *Hand2* without affecting the distal branchial arch expression. *Hand1*$^{NCKO/KO}$; *Hand2*$^{KO/+}$ mice were born at full term with expected Mendelian frequency, however, they died within 24 hours after birth because of failure to suckle. Gross

examination revealed a hypoplastic jaw with normal proximo-distal patterning and cleft palate, which are similar to, but milder than those of *Hand2*$^{BA/BA}$ mice. Similarly, all *Hand1*$^{NCKO/KO}$; *Hand2*$^{BA/BA}$ mice exhibited hypoplastic mandible and cleft palate and died within 24 hours of birth.

To further examine craniofacial structures in *Hand1*$^{NCKO/KO}$; *Hand2*$^{KO/+}$ and *Hand1*$^{NCKO/KO}$; *Hand2*$^{BA/BA}$ mice, we performed bone and cartilage staining on P1 pups. In wild-type animals, bilateral palatine processes extended horizontally and fused to form the secondary palate (dashed line in Fig. 2A). In contrast, the palatine processes of *Hand1*$^{NCKO/KO}$; *Hand2*$^{KO/+}$ and *Hand1*$^{NCKO/KO}$; *Hand2*$^{BA/BA}$ mice did not elevate to form the secondary palate (dashed line in Figs. 2B, D), as was observed in *Hand2*$^{BA/BA}$ mice (Fig. 2C). This causes the underlying presphenoid bone to be visible in the ventral view (arrows in Fig. 2B–D). The size of the mandible in *Hand1*$^{NCKO/KO}$; *Hand2*$^{KO/+}$ pups was smaller than that of wild-type (compare Fig. 2E and F), and *Hand1*$^{NCKO/KO}$; *Hand2*$^{BA/BA}$ pups developed a much smaller, deformed mandible compared with the rest of the mutants (Figs. 2F, G and H). In both *Hand1*$^{NCKO/KO}$; *Hand2*$^{KO/+}$ and *Hand1*$^{NCKO/KO}$; *Hand2*$^{BA/BA}$ mice, secondary structures derived from the most posterior segments of Meckel's cartilages developed normally as demonstrated by a lack of noticeable malformations in corresponding middle ear ossicles (data not shown). These data clearly indicate that there is a dosage effect of *Hand* genes on the development of subsets of cranial neural crest derivatives (Table 1).

Hand1 and midline defects

Careful examination of stained mandibular skeletal preparations revealed the distal symphysis of the mandible in wild type and *Hand2*$^{BA/BA}$ pups (Figs. 2E, G, dotted area). In contrast, *Hand1*$^{NCKO/KO}$; *Hand2*$^{KO/+}$ and *Hand1*$^{NCKO/KO}$; *Hand2*$^{BA/BA}$ pups developed a fused mandible due to the absence of symphysial cartilage (Figs. 2F, H, arrowhead). In addition, a single incisor developed at the midline of the distal tip of the mandible where the two halves were fused. The incisor abnormality was detected with complete penetrance in *Hand1*$^{NCKO/KO}$; *Hand2*$^{KO/+}$ pups. In *Hand1*$^{NCKO/KO}$; *Hand2*$^{BA/BA}$ pups, two lower incisors were occasionally found within the fused mandible (data not shown). Lower molars and upper teeth were normal in both mutants (data not shown). In addition to the incisor defect, we observed abnormal fusion of the hyoid and thyroid cartilage at the midline in *Hand1*$^{NCKO/KO}$; *Hand2*$^{KO/+}$ mutants, but not in *Hand2*$^{BA/BA}$ or *Hand1*$^{NCKO/KO}$; *Hand2*$^{BA/BA}$ pups (data not shown).

To better understand the nature of the lower incisor defect, we performed micro-CT analysis of the whole head from wild-type and *Hand1*$^{NCKO/KO}$; *Hand2*$^{KO/+}$ mutant pups. In the wild-type pup, two well-developed and separated incisors were detected at the distal (incisal) tip within the mandible (Fig. 3A), whereas a single, somewhat rectangularly-shaped incisor was found within the fused distal tip of the mandible in the mutant (Fig. 3B). Von Kossa staining of P1 wild-type mandible showed two distinct incisors distal-lateral to Meckel's cartilage surrounded by a thin layer of mineralized matrix and separated by well-developed cartilaginous symphysis (Fig. 3C, asterisk). Two separate incisors were also detected in the *Hand2*$^{BA/BA}$ pups, although the symphysis was smaller than that of wild-type (Fig. 3D, asterisk). In contrast, a single fused incisor with a common dental pulp was observed in both *Hand1*$^{NCKO/KO}$; *Hand2*$^{KO/+}$ (Fig. 3E) and *Hand1*$^{NCKO/KO}$; *Hand2*$^{BA/BA}$ pups (Fig. 3F). A markedly reduced symphysis was observed near the base of the incisor, occasionally embedded within the single incisor (Fig. 3H, arrow). H&E staining of transverse sections of P1 embryos revealed that polarized odontoblasts lined the pulp, and dentin and the enamel organ was well formed in wild-type embryos (Fig. 3G, inset). In the mutant, polarized odontoblasts and ameloblasts were observed and a dentin layer was formed, however, the enamel layer was severely reduced or defective (Fig. 3H, inset). In addition, the extrinsic muscle of the tongue, genioglossus, and

the geniohyoid muscle were also smaller, possessing fewer myofibers in the mutants than in the wild type mice (compare g and gh in Figs. 3I and J).

Changes in transcription factors implicated in tooth development in *Hand1*$^{NCKO/KO}$; *Hand2*$^{KO/+}$ embryos

To determine whether defects in the patterning of the odontogenic epithelium could account for the incisor fusion in *Hand1*$^{NCKO/KO}$; *Hand2*$^{KO/+}$ mandibles, we performed section *in situ* hybridization in E10.5 embryos and evaluated the expression of signaling molecules that induce the early patterning of the first branchial arch. The expression of *Shh* and *Wnt7b*, which are essential for specification of the oral epithelium, was unaffected in *HAND1*$^{NCKO/KO}$; *Hand2*$^{KO/+}$ embryos compared with wild-type embryos (Figs. 4A–D). *Bmp4* defines the incisor domain in the oral epithelium and no alteration of the expression domain of *Bmp4* was observed in *HAND1*$^{NCKO/KO}$; *Hand2*$^{KO/+}$ embryos (compare arrows in Figs. 4E, F). These observations suggest that compromized mesenchymal *Hand* expression does not affect specification of the odontogenic epithelium in mutant embryos.

Next, we examined by whole-mount *in situ* hybridization using E12.5 embryos whether transcription factors implicated in tooth organogenesis are altered or misexpressed in *Hand1*$^{NCKO/KO}$; *Hand2*$^{KO/+}$ and *Hand1*$^{NCKO/KO}$; *Hand2*$^{BA/BA}$ mutants, thus causing abnormal lower incisor development. Since *Hand1* and *Hand2* are not expressed in the oral epithelium and the defect is restricted to lower incisors, we first focused on genes expressed in the mesenchyme of the distal mandibular arch. *Pax9* marks prospective sites of odontogenesis prior to any morphological manifestation (Neubuser et al., 1995). *Pax9*$^{-/-}$ teeth proceed to the tooth bud stage but eventually arrest and result in agenesis (Peters et al., 1998). In wild-type embryos, *Pax9* showed restricted expression in the distal mesenchyme of the mandibular arch and in the maxillary process (Figs. 5A, a). In *Hand1*$^{NCKO/KO}$; *Hand2*$^{KO/+}$ and *Hand1*$^{NCKO/KO}$; *Hand2*$^{BA/BA}$ embryos, *Pax9* expression was unaffected in the aboral mesenchyme, however, a small portion of the *Pax9* expression domain between the lower incisor tooth buds was reduced (Figs. 5b, c, arrows).

Msx1 and *Msx2* are well-known BMP target genes and *Msx1* is downstream of *Hand2* in the ectomesenchyme of the mandibular arch (Semba et al., 2000; Thomas et al., 1998). In wild-type embryos, *Msx1* was expressed in the mesenchyme of the distal mandibular arch, maxillary arch and in the nasal process, and mutant embryos exhibited a similar pattern (Figs. 5D–F, d–f). *Msx2* was restricted to the region where prospective incisors form in the mandibular arch in the wild-type embryo (Fig. 5g, arrow). In mutant embryos, *Msx2* expression was significantly weaker, and the reduced distance between the two lower incisors was readily visible (Figs. 5h, I, arrows). These data suggest that *Hand1* and *Hand2* may be upstream of *Msx2* in the mandibular arch mesenchyme (Figs. 5G–I).

The position- and gene dosage-dependent lower incisor and mandible phenotype in *Hand* mutant mice share a striking similarity with that of *Prx1*$^{-/-}$; *Prx2*$^{-/-}$ mice (Lu et al., 1999; ten Berge et al., 1998; ten Berge et al., 2001). *Prx1* and *Prx2* belong to the paired-related homeobox gene family expressed in the craniofacial primordium, branchial arches and limb buds during embryogenesis (Cserjesi et al., 1992; Leussink et al., 1995). *Prx1*$^{-/-}$; *Prx2*$^{-/-}$ double homozygous neonates exhibit some novel defects that are not observed in single knockout mice, including a hypoplastic mandible with absent or only one lower incisor. Therefore, to determine if *Hand1* and *Hand2* are upstream of *Prx1* and *Prx2*, we examined expression of *Prx* genes in our mutant embryos. *Prx1* was expressed in the maxillary arch, vibrissae and the distal mesenchyme of the mandibular arch, and no difference was detected between the wild-type and mutant embryos (Figs. 5J–L, j–l). *Prx2* was expressed in more distal regions of the maxillary and mandibular arches compared to *Prx1* in the wild-type embryos

(Fig. 5m). While normal maxillary expression of *Prx2* was maintained in mutant embryos (Figs. 5N, O), the mandibular expression was reduced (Figs. 5n, o).

These results suggest that initial tooth organogenesis occurred normally in the mutant embryos; however, a reduction in total *Hand* gene dosage may have caused down-regulation of *Pax9*, *Msx2* and *Prx2* genes and lead to the developmental defect of the midline mesenchyme and/or lower incisor development. The possibility still exists that a loss of appropriate cells between the lower incisors altered the expression domains of these genes within the mandibular arch.

Defect of the distal midline mesenchyme in *Hand1*$^{NCKO/KO}$; *Hand2*$^{KO/+}$ mutant mice

To determine the onset of the fusion defect of mandible and incisors with respect to distal midline mesenchyme development in *Hand1*$^{NCKO/KO}$; *Hand2*$^{KO/+}$ and *Hand1*$^{NCKO/KO}$; *Hand2*$^{BA/BA}$ mutants, we focused on the phenotype of *Hand1*$^{NCKO/KO}$; *Hand2*$^{KO/+}$ embryos and performed whole-mount lacZ staining followed by serial sectioning. At E10.5, both *Hand1*$^{KO/+}$ control and *Hand1*$^{NCKO/KO}$; *Hand2*$^{KO/+}$ embryos contained lacZ-positive cells in the distal part of the mandibular arch and no difference was observed between the genotypes (data not shown). Next, we harvested mutant embryos between E11.5 and E14.5, the critical period of dental lamina formation through cap stage tooth formation, and compared them with *Hand1*$^{KO/+}$ control embryos. At E11.5, strong lacZ expression was observed in the midline mesenchyme extending from the mandibular component of the first branchial arch in the *Hand1*$^{KO/+}$ embryos (Fig. 6A). A slight reduction of the lacZ-positive mesenchyme was observed in *Hand1*$^{NCKO/KO}$; *Hand2*$^{KO/+}$ mutant (Fig. 6B). At E12.5, the dental lamina had proliferated and invaginated into the underlying mesenchyme in *Hand1*$^{KO/+}$ embryos (Fig. 6C, de). A lacZ-positive mesenchyme was well-developed and demarcated two prospective incisor tooth buds. In contrast, the invagination of the dental lamina was less distinct and lacZ-positive mesenchyme did not extend between the prospective incisor tooth buds in *Hand1*$^{NCKO/KO}$; *Hand2*$^{KO/+}$ embryos (Fig. 6D, arrow). At E13.5, a more localized thickening of the dental lamina and formation of the corresponding dental mesenchyme were observed in *Hand1*$^{KO/+}$ embryos (Fig. 6E). Strong lacZ expression was observed in the mesenchyme between the tooth buds and between and above the genioglossus muscles in the tongue. The dental mesenchyme was negative for lacZ (Fig. 6E, arrow). In mutant embryos, the two incisor tooth buds were fused and the lacZ-positive mesenchyme was no longer evident except in a small area aboral to the tooth bud (Fig. 6F). The lacZ staining was also significantly reduced in the mutant tongue (data not shown). At E14.5, cap-shaped incisor tooth buds were visible in control embryos (Fig. 6I, dotted area). The lacZ expression was most intense at the symphysis (Fig. 6G, arrow) and persisted along the distal-proximal axis (Figs. 6G, I, K). The site of fusion of Meckel's cartilage, as well as its surrounding perichondrium, was composed of both lacZ-positive and negative cells (Fig. 6I). The inter-dental mesenchyme, which extends toward the oral epithelium and separates the two incisors in control embryos was strongly positive for lacZ (Fig. 6I, arrow). Neural crest-derived dental mesenchyme where *Hand2* is expressed (Abe et al., 2002) was negative for lacZ (Fig. 6I, double arrows). In mutant embryos, the symphysis of Meckel's cartilage was markedly reduced in size and located aborally as indicated by the lacZ-positive area (Fig. 6H, arrow), and the two incisor primordia were fused near the oral base, giving rise to a fused incisor (Fig. 6J, I, dotted area). Abnormal blunting of the tip of Meckel's cartilage was also observed in the mutant (Fig. 6L, arrow).

To investigate the cellular mechanism of retarded growth of the distal midline mesenchyme in mutant embryos, we performed proliferation and apoptosis assays on E10.5 and E14.5 sections using anti-phosphorylated histone H3 immunostaining and TUNEL assay, respectively. No difference was observed in proliferation or apoptosis of mesenchymal cells between wild-type and *Hand1*$^{NCKO/KO}$; *Hand2*$^{KO/+}$ embryos at E10.5 (Supplemental Fig. 1A, B). At E14.5, we found a trend for increased apoptosis in the distal incisor portion of the mutant mandible,

however, it was not statistically significant (p=0.053, Supplemental Fig. 1B). No difference in proliferation was detected in the distal or proximal portion of the mandible at E14.5. These data indicate that *Hand* genes are not responsible for maintenance of cell numbers in the distal midline mesenchyme at early or late developmental stages, although the assessment of cell cycle length at E10.5 may reveal the underlying cause of growth defect of the midline mesenchyme.

Distal midline mesenchyme defect leads to premature ossification of the mandible in *Hand1*$^{NCKO/KO}$;*Hand2*$^{KO/+}$ mice

In the mandibular arch, the absence of ventrolateral *Hand2* expression or the reduction of *Hand2* in the entire *Hand2* expression domain, in combination with the loss of *Hand1*, resulted in the distal mesenchyme defect and eventually led to fusion of the hemi-mandibles and lower incisors. To gain mechanistic insight into the relationship between the distal mesenchyme and the abnormal fusion event during late embryosgenesis, we compared the development of the mandible in mutant embryos and wild-type embryos. Bone and cartilage staining of wild-type E14.5 embryos showed a well-developed distal symphysis of Meckel's cartilage (Fig. 7A, arrow), and mineralization of the membranous bone was observed along the body of the Meckel's cartilage (Fig. 7A, double arrows). In contrast, mutant embryos showed a proportionally small and flat distal tip of the Meckel's cartilage (Fig. 7B, arrow), and bone mineralization reached beyond the anterior part of the Meckel's cartilage (Fig. 7B, double arrows). Von Kossa staining of E14.5 wild-type and *Hand1*$^{NCKO/KO}$; *Hand2*$^{KO/+}$ embryos were consistent with bone staining; while the distal portions of Meckel's cartilage showed no signs of calcified matrix (Fig. 7C) and mineralization was evident only around the proximal portion of the Meckel's cartilage in wild-type embryos (Fig. 7E, arrow), deposition of calcified matrix was already observed lateral to the Meckel's cartilages throughout the proximal-distal axis in *Hand1*$^{NCKO/KO}$; *Hand2*$^{KO/+}$ embryos (Figs. 7D and F, arrows). Since *Hand2*$^{BA/BA}$ embryos, which showed more severe hypoplastic mandible (see Fig. 2G, Table 1), did not exhibit deposition of calcified matrix at the distal portion of the mandible (Suppplemental Figure 2) and did not develop fused mandible, increased deposition of calcified matrix in *Hand1*$^{NCKO/KO}$; *Hand2*$^{KO/+}$ embryos was not simply a consequence of the shortening of Meckel's cartilage. Rather, it was indicative of accelerated membranous ossification of the mandible.

During intramembranous bone development, proliferation of mesenchymal cells is followed by their commitment to become osteoprogenitor cells, which differentiate into pre-osteoblasts and then into bone matrix-forming mature osteoblasts. To determine if the premature deposition of bone matrix is attributable to defects in the differentiation of mutant osteoblasts, sections of E14.5 wild-type and *Hand1*$^{NCKO/KO}$; *Hand2*$^{KO/+}$ embryos were probed by radioactive *in situ* hybridization for markers of osteoblasts. In both wild-type and mutant mandibles, *collagen α1(I)* expression was detected surrounding the Meckel's cartilage as well as in the adjacent incipient intramembranous bone (Figs. 8A, B, arrow). On the other hand, osteocalcin expression, a late marker of osteoblast differentiation (Ducy et al., 1997), was markedly reduced in the mandibles of *Hand1*$^{NCKO/KO}$; *Hand2*$^{KO/+}$ embryos (compare Fig. 8C and D). The osteoblasts in the mutant bone were not terminally differentiated, yet seemed to be inappropriately active leading to a premature deposition of the bone matrix.

It is known that at the distal symphysial region of the mandible, chondrocytes within Meckel's cartilage undergo terminal differentiation and the cartilage is eventually replaced by bone tissues (Ishizeki et al., 1999). To determine if the hypoplasia of the distal symphysis of Meckel's cartilage observed in *Hand1*$^{NCKO/KO}$; *Hand2*$^{KO/+}$ embryos lead to a delay in chondrocyte maturation, we examined the expression of chondrocyte maturation markers. C*ollagen α1(II)*, a marker of proliferating and prehypertrophic chondrocytes, was expressed

in both wild-type and mutant embryos (Figs. 8E, F). However, *Ihh* (Indian hedgehog) and *collagen α1(X)*, a specific marker of pre-hypertrophic chondrocytes and hypertrophic chondrocytes, respectively, was absent in mutant embryos (Figs 8G–J). Considering that *Hand1* was mainly expressed in the midline between the Meckel's cartilages in wild-type embryos (Fig. 8K), and both *Hand1* and *Hand2* were expressed only in subsets of cells in Meckel's cartilage symphysis (Ruest et al., 2003), the defect may be secondary to a retarded growth of midline mesenchyme at an earlier developmental stage. However, a direct role of *Hand* genes in terminal differentiation of Meckel's chondrocytes needs to be examined.

Discussion

In the present study, we performed tissue specific ablation in mice of the *Hand1* gene in combination with various mutant alleles of *Hand2*. We show that growth of the distal midline mesenchyme of the first branchial arch, which develops into the interdental mesenchyme and distal symphysis of Meckel's cartilage, is highly sensitive to dosage of the *Hand* genes. Secondary to the loss of distal midline mesenchyme, terminal differentiation of chondrocytes in Meckel's cartilage symphysis is affected and membranous ossification of the mandible becomes dysregulated, which together impair the coordinated growth of lower incisors.

Redundant roles of *Hand* genes in development of the distal midline mesenchyme of the mandibular arch

In the branchial arches, the *Hand1* domain is completely included in the *Hand2* domain, and deletion of *Hand1* in the first and second branchial arches in $Hand1^{NCKO/KO}$ mice was not sufficient to cause developmental defects. The overlapping expression domains of *Hand1* and *Hand2* and a highly conserved sequence in the HLH region of the two genes strongly suggest that *Hand2* compensates for loss of *Hand*1. Indeed, removing one copy of *Hand2* or deleting the ventrolateral branchial arch expression of *Hand2* in conjunction with branchial arch deletion of *Hand1* evoked a novel phenotype, perturbing the development of distal midline mesenchyme. The synergistic effect of *Hand1* and *Hand2* has been observed during cardiac development (McFadden et al., 2005). In cardiac-specific deletion mutants of *Hand1*, expansion of the left ventricle where *Hand1* is predominantly expressed, is perturbed in a *Hand2* gene dose-sensitive manner, causing a more severe phenotype than seen in single-knockout embryos. The requirement of *Hand* gene dosage for proper development of the distal craniofacial mesenchyme suggests that *Hand1* and *Hand2* redundantly regulate the same sets of target genes in the branchial arches. Knock-in studies in which the *Hand2* locus is replaced with *Hand1* and vise versa will be required to establish redundant roles of *Hand in vivo*.

Our findings shed light on the previously unrecognized role of *Hand* genes in the regulation of inter-dental mesenchyme development. In contrast to a previous report showing that increased apoptosis was responsible for hypoplastic branchial arch in *Hand2*-null embryos (Thomas et al., 1998), we failed to detect significant differences in proliferation or apoptosis between wild-type and *Hand1/2* compound mutants at E10.5 and E14.5. However, this does not exclude the possibility that a slight decrease of proliferation and/or a gradual increase of apoptosis that was not detected during these time windows, may be responsible for compromised distal midline mesenchyme growth. It is recently reported that *Hand1* regulates proliferation of cardiomyocytes by controlling cyclinD1 and cyclin dependent kinase 4 (Risebro et al., 2006). In the absence of *Hand1*, proliferation of cardiomyocytes in the distal outflow tract was decreased and myocytes undertook differentiation pathway. Therefore, it is plausible that *Hand* genes are involved in the initial proliferation of specific ectomesenchymal cell populations at the distal midline. Second possibility is that loss of *Hand* expression in the distal midline alters the boundaries of transcription factors expressed in adjacent domains of the branchial arch. For instance, *Hand2* restricts dorsal expression of *eng2* and dorsal-lateral

expression of *bapx1* (=Nkx3.2) to specify ventral branchial cartilages during zebrafish development (Miller et al., 2003). Therefore, the spatial relationship of *HAND* expression domain with that of other transcription factors may be critical for regulation of transcriptional circuitry during midline mesenchyme development.

In *Hand* compound mutants, *Shh*, *Wnt7b*, *Fgf8*, *Patched* and *Msx1* were expressed normal levels and a *Bmp4*-positive incisor domain was not disrupted in E10.5 mutant embryos, suggesting that *Hand1* and *Hand2* are not involved in specification of the oral epithelial boundary between incisors and molars. Rather, it seems that lower incisors were fused due to hypoplastic inter-dental mesenchyme. It has been reported that several key molecules known to regulate development of the distal midline of the mandibular arch, including *Hand2*, *Dlx3*, *Alx4*, *Pitx1* and *BMP7*, are markedly down-regulated in $Dlx5^{-/-};Dlx6^{-/-}$ embryos (Depew et al., 2002). In these mutants, Meckel's cartilage and the mandible are absent and transformation of the mandible to maxilla is observed. Lower incisors do form, but, they are not associated with each other and occasionally accompanied by a remnant of the distal midline cartilaginous structure. In *Hand* mutant embryos, it seems that the growth of the distal mesenchyme affects normal positioning of the incisors by allowing a direct contact of two apposing dental buds. Finally, it is possible that the inter-dental mesenchyme produces inhibitory signals that prevent fusion of the incisor buds.

Loss of *Hand* genes affects terminal differentiation of the Meckel's cartilage symphysis and ossification of the mandible

In $Hand1^{NCKO/KO}$; $Hand2^{KO/+}$ embryos, hypoplasia of the distal midline mesenchyme was evident as early as E11.5. Later at E14.5, chondrocytes within the distal symphysis of Meckel's cartilage failed to express the pre-hypertrophic chondrocyte marker *Ihh* and the hypertrophic chondrocyte marker *Collagen α1(X)* (Kronenberg, 2003). Secretion of Ihh tightly controls chondrocyte hypertrophy and differentiation, and *Ihh*-null mice exhibit initial delay in the formation of hypertrophic chondrocytes (St-Jacques et al., 1999; Vortkamp et al., 1996). An overlap in the expression of *Collagen α1 (II)*, *Ihh* and *Collagen α1(X)* in wild-type Meckel's cartilage indicates that these chondrocytes are in a transition between the proliferating and hypertrophic stages. In contrast, lack of expression of *Ihh* and *Collagen α1(X)* in mutant chondrocytes suggests that the terminal differentiation of chondrocytes is affected.

We also found that osteoblasts surrounding Meckel's cartilage symphysis were prematurely active in *Hand* mutants, indicated by accelerated deposition of calcified matrix, the presence of *Collagen α1(I)*, an early marker for osteoblast differentiation, and the absence of *Osteocalcin*, a marker for mature osteoblasts. Production of type I collagen is one of the earliest events associated with osteoblast differentiation (Franceschi and Iyer, 1992). Osteocalcin, a marker of terminally differentiated osteoblasts (Ducy and Karsenty, 1995), inhibits the function of osteoblasts, as *osteocalcin* mutant mice exhibit an increase in bone formation (Ducy et al., 1996). Thus, in *Hand* mutant embryos, although prematurely active osteocytes did not undergo excessive proliferation nor exhibit resistance to apoptosis during the formation of the mandible, they contributed to premature deposition of bone matrix.

Taken together, these findings suggest the possibility that impaired chondrocyte differentiation within the Meckel's symphysis induces a compensatory increase in intramembranous bone formation in the mandible at the distal tip, leading to the fused mandibles and a single incisor. Alternatively, Hands may regulate the activity of mandibular osteoblasts. It is also possible that secreted factor(s) from the symphysis may regulate the timing and the degree of intramembranous ossification of the mandible.

In *Hand2*-null mutant zebrafish, while dorsal cartilages were well-patterned, anterior ventral cartilages were almost absent, and upper jaw joints were connected by a cartilaginous bridge

at the midline (Miller et al., 2003). Excess and ectopic expression of *Msx* genes (*Msxe* and *Msxb*), which depend on upstream ET-1 signaling, was thought to prevent ventral arch neural crest cell differentiation into chondrocytes (Miller et al., 2000; Miller et al., 2003). It is therefore interesting to consider whether the defect of chondrocyte differentiation reflects a direct role of *Hand* genes, or whether it is mediated through an inhibitory factors that are suppressed by *Hand* genes during chondrocyte differentiation.

Implications

Craniofacial tissue boundaries are established by specific expression of transcription factors and growth factors within the developing branchial arches. The present study defines a *Hand*-sensitive distal sub-domain within the mandibular arch demarcated by overlapping expression of *Hand1* and *Hand2*. Our study also demonstrates that *Hand* genes are critical for the development of distal midline mesenchyme derivatives including the distal symphysis of Meckel's cartilage and inter-dental mesenchyme. Identification of direct targets of *Hand* genes as well as enhancer(s) that drives *Hand* expression in the distal mesenchyme will facilitate dissection of the genetic network involved in craniofacial development.

Supplementary Material

Refer to Web version on PubMed Central for supplementary material.

Acknowledgments

We thank members of the Pathology Core Laboratory at the University of Texas Southwestern Medical Center for excellent histological preparations, Mei Xin for technical assistance and Drs. Eric Small and David Clouthier for a critical reading of the manuscript. We also thank Lydia Malynowsky and Jean-Sebastien Binette of McGill University for their excellent technical assistance with the histology and the micro-computed tomography, respectively. This work was supported by the NIH (E.N.O.), the Donald W. Raynolds Clinical Cardiovascular Research Center (E.N.O.), the March of Dimes Birth Defect Foundation (H.Y.), and the Canadian Institutes of Health Research (M.D.M.). Noriko Funato was supported by the JSPS Postdoctoral Fellowships for Research Abroad 2005.

References

Abe M, Tamamura Y, Yamagishi H, Maeda T, Kato J, Tabata MJ, Srivastava D, Wakisaka S, Kurisu K. Tooth-type specific expression of dHAND/Hand2: possible involvement in murine lower incisor morphogenesis. Cell Tissue Res 2002;310:201–212. [PubMed: 12397375]

Aigner T, Dietz U, Stoss H, von der Mark K. Differential expression of collagen types I, II, III, and X in human osteophytes. Lab Invest 1995;73:236–243. [PubMed: 7637324]

Akiyama H, Shigeno C, Iyama K, Ito H, Hiraki Y, Konishi J, Nakamura T. Indian hedgehog in the late-phase differentiation in mouse chondrogenic EC cells, ATDC5: upregulation of type X collagen and osteoprotegerin ligand mRNAs. Biochem Biophys Res Commun 1999;257:814–820. [PubMed: 10208865]

Chai Y, Jiang X, Ito Y, Bringas P Jr, Han J, Rowitch DH, Soriano P, McMahon AP, Sucov HM. Fate of the mammalian cranial neural crest during tooth and mandibular morphogenesis. Development 2000;127:1671–1679. [PubMed: 10725243]

Chai Y, Maxson RE Jr. Recent advances in craniofacial morphogenesis. Dev Dyn 2006;235:2353–2375. [PubMed: 16680722]

Clouthier DE, Williams SC, Yanagisawa H, Wieduwilt M, Richardson JA, Yanagisawa M. Signaling pathways crucial for craniofacial development revealed by endothelin-A receptor-deficient mice. Dev Biol 2000;217:10–24. [PubMed: 10625532]

Cserjesi P, Brown D, Lyons GE, Olson EN. Expression of the novel basic helix-loop-helix gene eHAND in neural crest derivatives and extraembryonic membranes during mouse development. Dev Biol 1995;170:664–678. [PubMed: 7649392]

Cserjesi P, Lilly B, Bryson L, Wang Y, Sassoon DA, Olson EN. MHox: a mesodermally restricted homeodomain protein that binds an essential site in the muscle creatine kinase enhancer. Development 1992;115:1087–1101. [PubMed: 1360403]

Depew MJ, Lufkin T, Rubenstein JL. Specification of jaw subdivisions by Dlx genes. Science 2002;298:381–385. [PubMed: 12193642]

Ducy P, Desbois C, Boyce B, Pinero G, Story B, Dunstan C, Smith E, Bonadio J, Goldstein S, Gundberg C, et al. Increased bone formation in osteocalcin-deficient mice. Nature 1996;382:448–452. [PubMed: 8684484]

Ducy P, Karsenty G. Two distinct osteoblast-specific cis-acting elements control expression of a mouse osteocalcin gene. Mol Cell Biol 1995;15:1858–1869. [PubMed: 7891679]

Ducy P, Zhang R, Geoffroy V, Ridall AL, Karsenty G. Osf2/Cbfa1: a transcriptional activator of osteoblast differentiation. Cell 1997;89:747–754. [PubMed: 9182762]

Echelard Y, Epstein DJ, St-Jacques B, Shen L, Mohler J, McMahon JA, McMahon AP. Sonic hedgehog, a member of a family of putative signaling molecules, is implicated in the regulation of CNS polarity. Cell 1993;75:1417–1430. [PubMed: 7916661]

Firulli AB, McFadden DG, Lin Q, Srivastava D, Olson EN. Heart and extra-embryonic mesodermal defects in mouse embryos lacking the bHLH transcription factor Hand1. Nat Genet 1998;18:266–270. [PubMed: 9500550]

Franceschi RT, Iyer BS. Relationship between collagen synthesis and expression of the osteoblast phenotype in MC3T3-E1 cells. J Bone Miner Res 1992;7:235–246. [PubMed: 1373931]

Goodrich LV, Johnson RL, Milenkovic L, McMahon JA, Scott MP. Conservation of the hedgehog/patched signaling pathway from flies to mice: induction of a mouse patched gene by Hedgehog. Genes Dev 1996;10:301–312. [PubMed: 8595881]

Hardcastle Z, Mo R, Hui CC, Sharpe PT. The Shh signalling pathway in tooth development: defects in Gli2 and Gli3 mutants. Development 1998;125:2803–2811. [PubMed: 9655803]

Ishizeki K, Saito H, Shinagawa T, Fujiwara N, Nawa T. Histochemical and immunohistochemical analysis of the mechanism of calcification of Meckel's cartilage during mandible development in rodents. J Anat 1999;194(Pt 2):265–277. [PubMed: 10337959]

Jegalian BG, De Robertis EM. Homeotic transformations in the mouse induced by overexpression of a human Hox3.3 transgene. Cell 1992;71:901–910. [PubMed: 1360874]

Jeong J, Mao J, Tenzen T, Kottmann AH, McMahon AP. Hedgehog signaling in the neural crest cells regulates the patterning and growth of facial primordia. Genes Dev 2004;18:937–951. [PubMed: 15107405]

Jiang X, Rowitch DH, Soriano P, McMahon AP, Sucov HM. Fate of the mammalian cardiac neural crest. Development 2000;127:1607–1616. [PubMed: 10725237]

Jones CM, Lyons KM, Hogan BL. Involvement of Bone Morphogenetic Protein-4 (BMP-4) and Vgr-1 in morphogenesis and neurogenesis in the mouse. Development 1991;111:531–542. [PubMed: 1893873]

Kronenberg HM. Developmental regulation of the growth plate. Nature 2003;423:332–336. [PubMed: 12748651]

Leussink B, Brouwer A, el Khattabi M, Poelmann RE, Gittenberger-de Groot AC, Meijlink F. Expression patterns of the paired-related homeobox genes MHox/Prx1 and S8/Prx2 suggest roles in development of the heart and the forebrain. Mech Dev 1995;52:51–64. [PubMed: 7577675]

Lu MF, Cheng HT, Lacy AR, Kern MJ, Argao EA, Potter SS, Olson EN, Martin JF. Paired-related homeobox genes cooperate in handplate and hindlimb zeugopod morphogenesis. Dev Biol 1999;205:145–157. [PubMed: 9882503]

Matalova E, Tucker AS, Sharpe PT. Death in the life of a tooth. J Dent Res 2004;83:11–16. [PubMed: 14691106]

McFadden DG, Barbosa AC, Richardson JA, Schneider MD, Srivastava D, Olson EN. The Hand1 and Hand2 transcription factors regulate expansion of the embryonic cardiac ventricles in a gene dosage-dependent manner. Development 2005;132:189–201. [PubMed: 15576406]

McFadden DG, Charite J, Richardson JA, Srivastava D, Firulli AB, Olson EN. A GATA-dependent right ventricular enhancer controls dHAND transcription in the developing heart. Development 2000;127:5331–5341. [PubMed: 11076755]

Meyers EN, Martin GR. Differences in left-right axis pathways in mouse and chick: functions of FGF8 and SHH. Science 1999;285:403–406. [PubMed: 10411502]

Miletich I, Sharpe PT. Neural crest contribution to mammalian tooth formation. Birth Defects Res C Embryo Today 2004;72:200–212. [PubMed: 15269893]

Miller CT, Schilling TF, Lee K, Parker J, Kimmel CB. sucker encodes a zebrafish Endothelin-1 required for ventral pharyngeal arch development. Development 2000;127:3815–3828. [PubMed: 10934026]

Miller CT, Yelon D, Stainier DY, Kimmel CB. Two endothelin 1 effectors, hand2 and bapx1, pattern ventral pharyngeal cartilage and the jaw joint. Development 2003;130:1353–1365. [PubMed: 12588851]

Neubuser A, Koseki H, Balling R. Characterization and developmental expression of Pax9, a paired-box-containing gene related to Pax1. Dev Biol 1995;170:701–716. [PubMed: 7649395]

Opstelten DJ, Vogels R, Robert B, Kalkhoven E, Zwartkruis F, de Laaf L, Destree OH, Deschamps J, Lawson KA, Meijlink F. The mouse homeobox gene, S8, is expressed during embryogenesis predominantly in mesenchyme. Mech Dev 1991;34:29–41. [PubMed: 1680375]

Parr BA, Shea MJ, Vassileva G, McMahon AP. Mouse Wnt genes exhibit discrete domains of expression in the early embryonic CNS and limb buds. Development 1993;119:247–261. [PubMed: 8275860]

Peters H, Neubuser A, Kratochwil K, Balling R. Pax9-deficient mice lack pharyngeal pouch derivatives and teeth and exhibit craniofacial and limb abnormalities. Genes Dev 1998;12:2735–2747. [PubMed: 9732271]

Ramaesh T, Bard JB. The growth and morphogenesis of the early mouse mandible: a quantitative analysis. J Anat 2003;203:213–222. [PubMed: 12924821]

Riddle RD, Johnson RL, Laufer E, Tabin C. Sonic hedgehog mediates the polarizing activity of the ZPA. Cell 1993;75:1401–1416. [PubMed: 8269518]

Risebro CA, Smart N, Dupays L, Breckenridge R, Mohun TJ, Riley PR. Hand1 regulates cardiomyocyte proliferation versus differentiation in the developing heart. Development 2006;133:4595–4606. [PubMed: 17050624]

Ruest LB, Dager M, Yanagisawa H, Charite J, Hammer RE, Olson EN, Yanagisawa M, Clouthier DE. dHAND-Cre transgenic mice reveal specific potential functions of dHAND during craniofacial development. Dev Biol 2003;257:263–277. [PubMed: 12729557]

Sakakura Y, Tsuruga E, Irie K, Hosokawa Y, Nakamura H, Yajima T. Immunolocalization of receptor activator of nuclear factor-kappaB ligand (RANKL) and osteoprotegerin (OPG) in Meckel's cartilage compared with developing endochondral bones in mice. J Anat 2005;207:325–337. [PubMed: 16191162]

Sasaki T, Ito Y, Xu X, Han J, Bringas P Jr, Maeda T, Slavkin HC, Grosschedl R, Chai Y. LEF1 is a critical epithelial survival factor during tooth morphogenesis. Dev Biol 2005;278:130–143. [PubMed: 15649466]

Selleck MA, García-Castro MI, Artinger KB, Bronner-Fraser M. Effects of Shh and Noggin on neural crest formation demonstrate that BMP is required in the neural tube but not ectoderm. Development 1999;125:4919–4930. [PubMed: 9811576]

Semba I, Nonaka K, Takahashi I, Takahashi K, Dashner R, Shum L, Nuckolls GH, Slavkin HC. Positionally-dependent chondrogenesis induced by BMP4 is co-regulated by Sox9 and Msx2. Dev Dyn 2000;217:401–414. [PubMed: 10767084]

Shelton JM, Lee MH, Richardson JA, Patel SB. Microsomal triglyceride transfer protein expression during mouse development. J Lipid Res 2000;41:532–537. [PubMed: 10744773]

Shin CH, Liu ZP, Passier R, Zhang CL, Wang DZ, Harris TM, Yamagishi H, Richardson JA, Childs G, Olson EN. Modulation of cardiac growth and development by HOP, an unusual homeodomain protein. Cell 2002;110:725–735. [PubMed: 12297046]

Sohal GS, Ali MM, Ali AA, Dai D. Ventrally emigrating neural tube cells contribute to the formation of Meckel's and quadrate cartilage. Dev Dyn 1999;216:37–44. [PubMed: 10474164]

Srivastava D, Cserjesi P, Olson EN. A subclass of bHLH proteins required for cardiac morphogenesis. Science 1995;270:1995–1999. [PubMed: 8533092]

Srivastava D, Thomas T, Lin Q, Kirby ML, Brown D, Olson EN. Regulation of cardiac mesodermal and neural crest development by the bHLH transcription factor, dHAND. Nat Genet 1997;16:154–160. [PubMed: 9171826]

St-Jacques B, Hammerschmidt M, McMahon AP. Indian hedgehog signaling regulates proliferation and differentiation of chondrocytes and is essential for bone formation. Genes Dev 1999;13:2072–2086. [PubMed: 10465785]

Stottmann RW, Anderson RM, Klingensmith J. The BMP antagonists Chordin and Noggin have essential but redundant roles in mouse mandibular outgrowth. Dev Biol 2001;240:457–473. [PubMed: 11784076]

ten Berge D, Brouwer A, Korving J, Martin JF, Meijlink F. Prx1 and Prx2 in skeletogenesis: roles in the craniofacial region, inner ear and limbs. Development 1998;125:3831–3842. [PubMed: 9729491]

ten Berge D, Brouwer A, Korving J, Reijnen MJ, van Raaij EJ, Verbeek F, Gaffield W, Meijlink F. Prx1 and Prx2 are upstream regulators of sonic hedgehog and control cell proliferation during mandibular arch morphogenesis. Development 2001;128:2929–2938. [PubMed: 11532916]

Thomas T, Kurihara H, Yamagishi H, Kurihara Y, Yazaki Y, Olson EN, Srivastava D. A signaling cascade involving endothelin-1, dHAND and msx1 regulates development of neural-crest-derived branchial arch mesenchyme. Development 1998;125:3005–3014. [PubMed: 9671575]

Trichilis A, Wroblewski J. Expression of p53 and hsp70 in relation to apoptosis during Meckel's cartilage development in the mouse. Anat Embryol (Berl) 1997;196:107–113. [PubMed: 9278155]

Tucker A, Sharpe P. The cutting-edge of mammalian development; how the embryo makes teeth. Nat Rev Genet 2004;5:499–508. [PubMed: 15211352]

Vortkamp A, Lee K, Lanske B, Segre GV, Kronenberg HM, Tabin CJ. Regulation of rate of cartilage differentiation by Indian hedgehog and PTH-related protein. Science 1996;273:613–622. [PubMed: 8662546]

Yanagisawa H, Clouthier DE, Richardson JA, Charite J, Olson EN. Targeted deletion of a branchial arch-specific enhancer reveals a role of dHAND in craniofacial development. Development 2003;130:1069–1078. [PubMed: 12571099]

Yanagisawa H, Yanagisawa M, Kapur RP, Richardson JA, Williams SC, Clouthier DE, de Wit D, Emoto N, Hammer RE. Dual genetic pathways of endothelin-mediated intercellular signaling revealed by targeted disruption of endothelin converting enzyme-1 gene. Development 1998;125:825–836. [PubMed: 9449665]

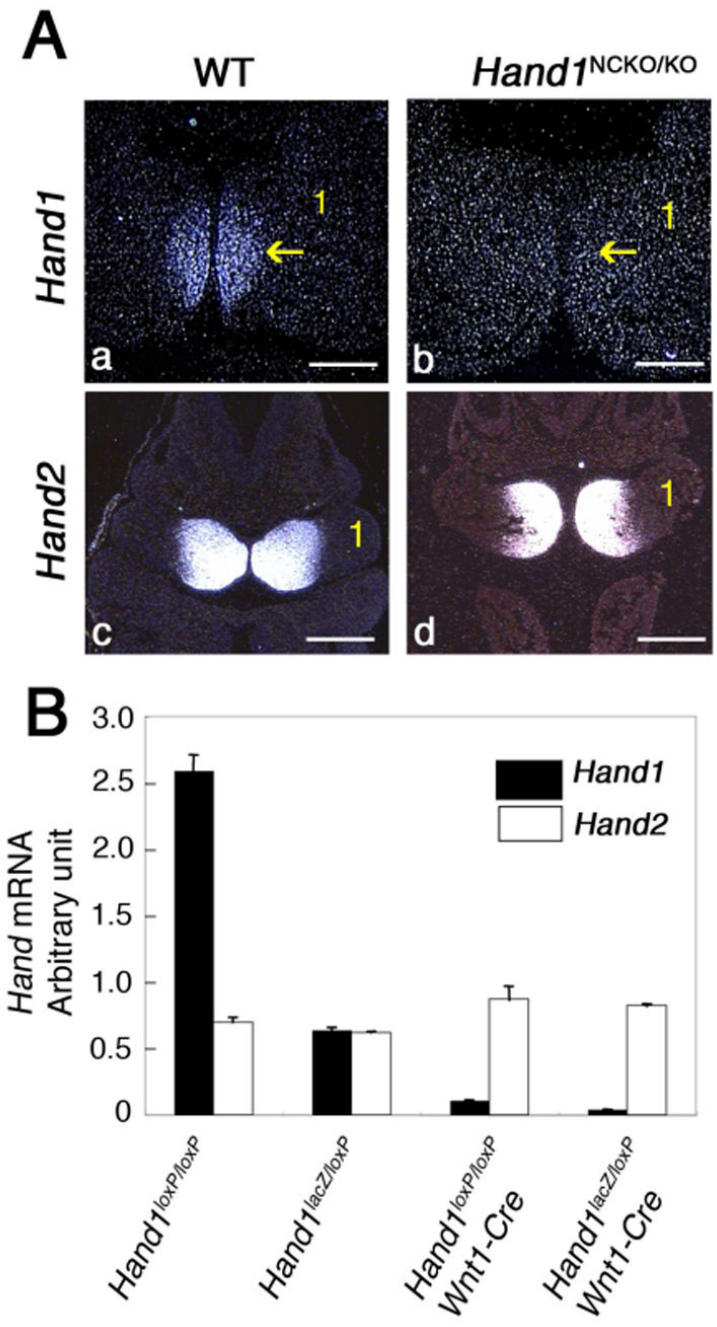

Figure 1. Neural crest-specific Cre-mediated recombination of *Hand1*

(A). Expression of *Hand1* and *Hand2* was examined by *in situ* hybridization of transverse sections of E10.5 wild-type (panels a, c) and *Hand1*$^{NCKO/KO}$ (panels b, d) embryos. *Hand1* expression seen in the distal part of the mandibular arch (panel a, arrow) is absent in the mutant (panel b, arrow); *Hand2* expression is unaffected (panel d). Bars indicate 200 μm (panels a, b) and 400 μm (panels c, d). 1; first mandibular arch.

(B). Detection of *Hand1* and *Hand2* by real-time RT-PCR using RNA extracted from mandibular and second branchial arches of *Hand1*$^{loxP/loxP}$, *Hand1*$^{lacZ/loxp}$ and *Hand1*$^{NCKO/KO}$ (*Hand1*$^{loxP/loxP}$; *Wnt1::Cre* and *Hand1*$^{lacZ/loxP}$;*Wnt1::Cre*) embryos at E10.5. Values are normalized to *18S* expression. *Hand1* expression is almost undetectable in the

mutants, whereas *Hand2* expression is maintained in embryos from all genotypes. Bars are means ± SD.

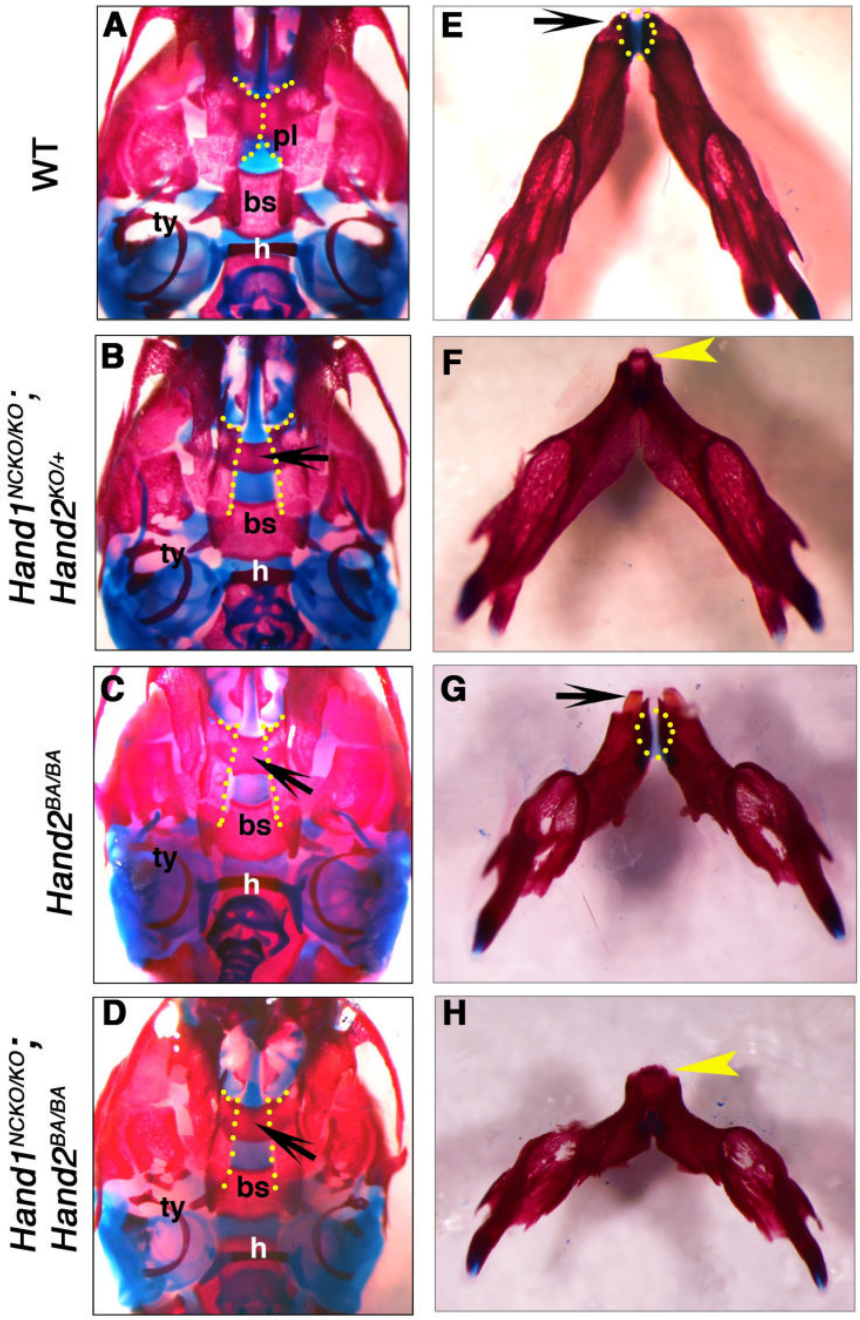

Figure 2. Craniofacial defects in P1 mice with compound mutations in *Hand1* and *Hand2*

Bone and cartilage staining of wild-type (A, E), *Hand1*^{NCKO}; *Hand2*$^{KO/+}$ (B, F), *Hand2*$^{BA/BA}$ (C, G) and *Hand1*^{NCKO}; *Hand2*$^{BA/BA}$ (D, H) mutant mice are shown. **(A–D)** Ventral views of the skull. Fusion of the bilateral palatine processes observed in the wild-type mouse (A, dashed line) is absent in the mutants (B-D, dashed line). Underlying presphenoid bone is visible in the mutants (arrows in B–D). **(E–H)** Ventral views of the mandible. The mandible of the mutants (F–G) is shorter and deformed. The angle between the left and right mandible is wider compared to the wild-type mouse (E). Note that the deformity of the mandible increases as total *Hand1* and *Hand2* gene dosage decreases. Wild-type (E) and *Hand2*$^{BA/BA}$ (G) mice show two incisors at the distal tip (arrow), whereas the mandible and

lower incisors are fused in *Hand1*^{NCKO}; *Hand2*$^{KO/+}$ (F) and *Hand1*^{NCKO}; *Hand2*$^{BA/BA}$ (H) mice (arrowhead). Note that the distal symphysis of the mandible is present in the wild-type and *Hand2*$^{BA/BA}$ mice (E, G, dotted area) but absent in the compound mutants (F, H).

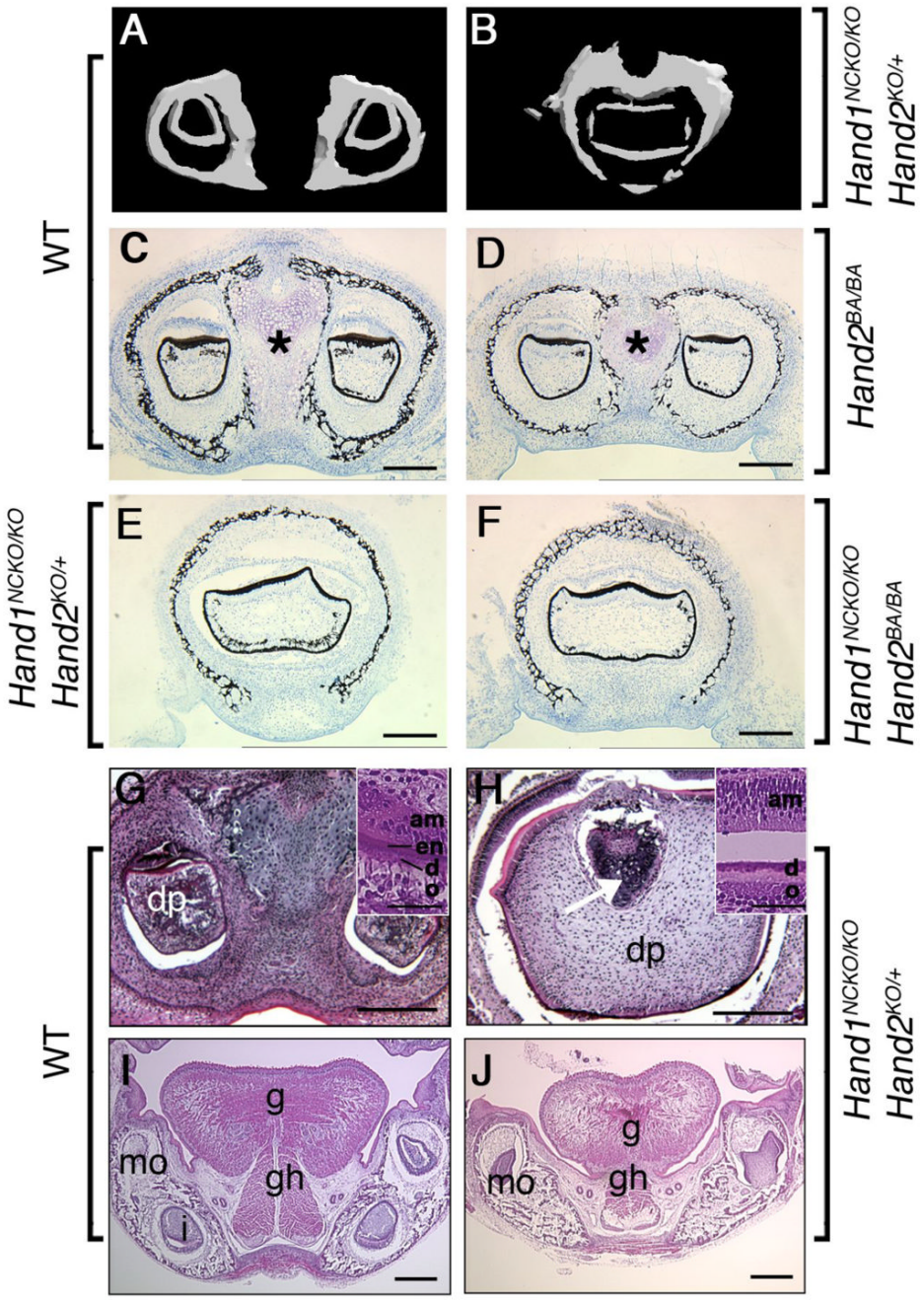

Figure 3. Abnormal fusion of the lower incisors

(A, B) Micro-CT analysis of the lower incisors in P1 embryos. In wild-type embryo (A), two lower incisors are located within the mandible. In contrast, a large deformed single incisor is observed within the fused mandible of the mutant (B). **(C–F)** Von Kossa staining of coronal sections of the mandible in plastic-embedded wild-type (C), *Hand2*$^{BA/BA}$ (D), *Hand1*$^{NCKO/KO}$;*Hand2*$^{KO/+}$ (E) and *Hand1*$^{NCKO/KO}$;*Hand2*$^{BA/BA}$ (F) embryos. In wild-type embryos, a well-developed distal symphysis of Meckel's cartilage is observed (asterisk in C). The symphysis is much smaller in the *Hand2*$^{BA/BA}$ mutant (asterisk in D) and becomes undetectable in *Hand1*$^{NCKO/KO}$;*Hand2*$^{KO/+}$ and *Hand1*$^{NCKO/KO}$;*Hand2*$^{BA/BA}$ embryos (E, F). Fused incisors are seen in mutant embryos (E, F). (G–J) H&E staining of coronal paraffin

sections of P1 wild-type (G, I) and *Hand1*$^{NCKO/KO}$;*Hand2*$^{KO/+}$ (H, J) embryos. **(G, H)** In wild-type embryos (G), two incisors with normal cytodifferentiation, including dental papilla (dp), odontoblasts (o), dentin (d), enamel (en) and ameloblasts (am) are observed (inset in G). In the mutant (H), a large fused incisor is observed, and the enamel layer is absent (inset in H). The distal symphysis is embedded in the dental papilla (H, arrow). **(I, J)** Well-developed extrinsic muscles (g; genioglossus, gh; geniohyoid) are observed in the tongue of wild-type embryos (I). In the mutant (J), muscle fibers are sparse and hypoplastic. Bars indicate 100 μm (C–J) and 40 μm (inset in G and H). mo; molar, i; incisor.

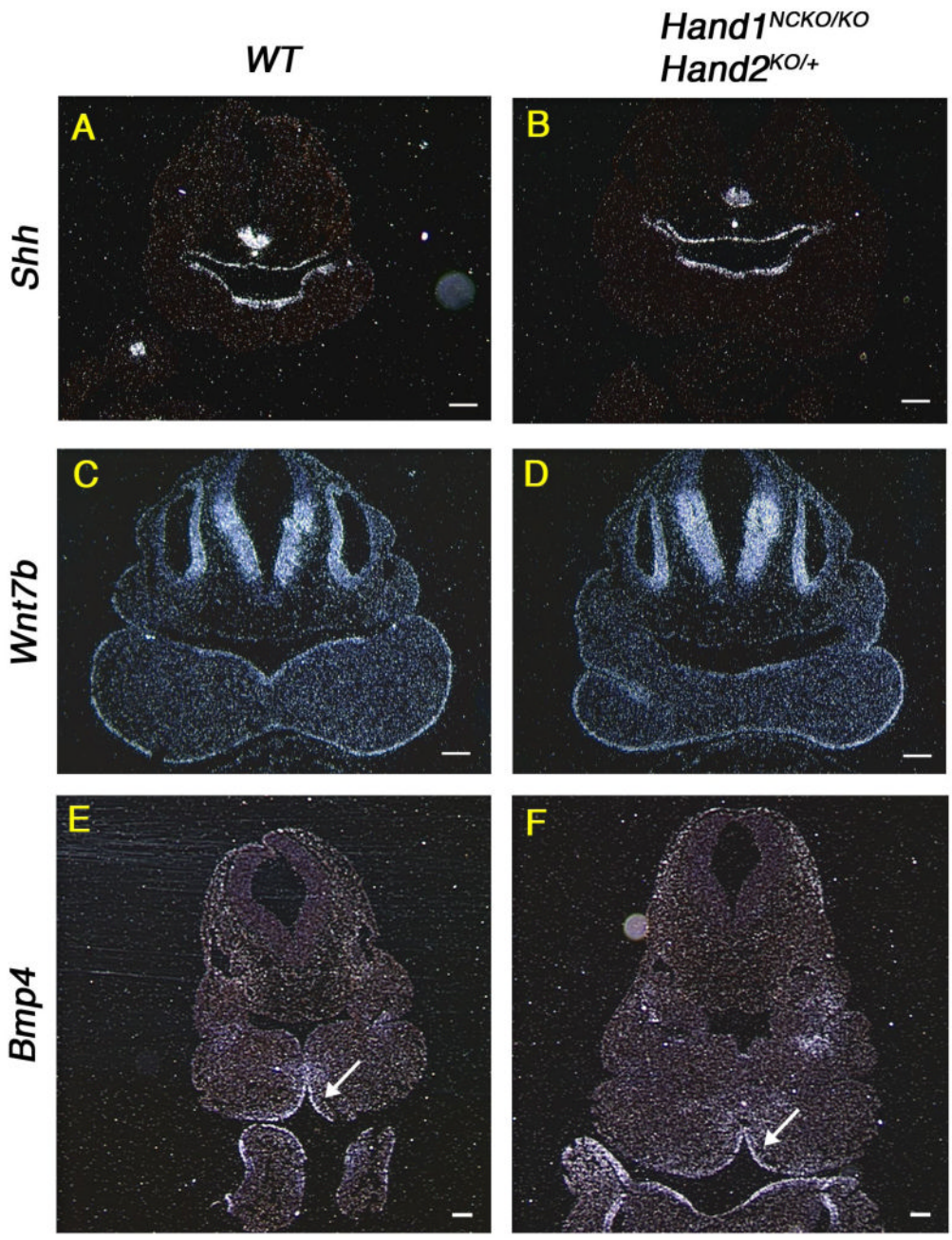

Figure 4. Normal specification of the odontogenic epithelium in E10.5 mutant embryos

In situ hybridization of transverse sections from E10.5 wild-type (A, C, E) and *Hand1*$^{NCKO/KO}$;*Hand2*$^{KO/+}$ (B, D, F) embryos probed with *Shh* (A, B), *Wnt7b* (C, D) and *Bmp4* (E, F). Arrow in E and F indicates that a *Bmp4* domain is not altered in the mutant embryo compared with wild-type embryo. Bars indicate 100 μm.

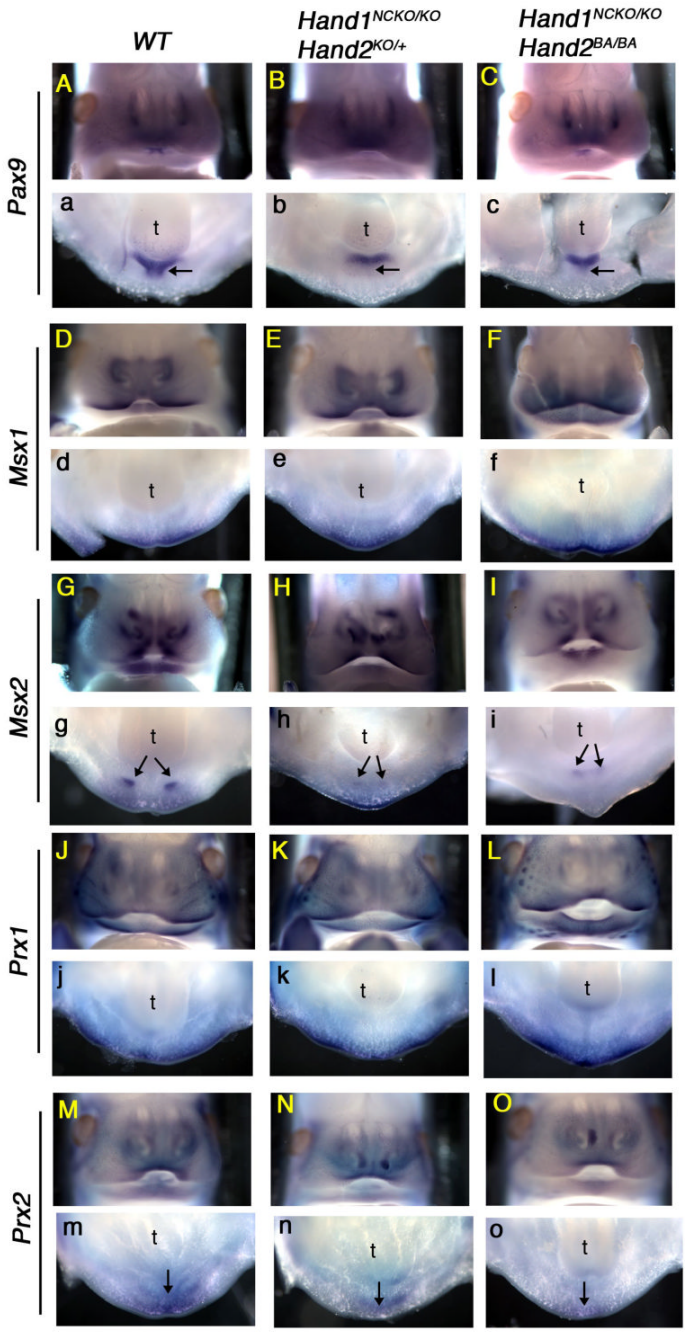

Figure 5. Dysregulation of branchial arch genes in embryos with compound mutations in *Hand1* and *Hand2*

Whole-mount *in situ* hybridization was performed in E12.5 wild-type (A, a, D, d, G, g, J, j, M, m), *Hand1*$^{NCKO/KO}$;*Hand2*$^{KO/+}$ (B, b, E, e, H, h, K, k, N, n) and *Hand1*$^{NCKO/KO}$;*Hand2*$^{BA/BA}$ (C, c, F, f, I, i, L, l, O, o) embryos. Frontal views (upper case) and transverse oral views (lower case) are shown. *Pax9* is expressed in the dental and inter-dental (arrow in a) mesenchyme of the wild-type embryos, however, inter-dental expression is absent in both mutant embryos (arrows in b, c). *Msx2* is expressed in the incisors (arrows in g) and *Prx2* is expressed in the distal midline mesenchyme of wild-type embryos (arrow in m).

In both mutants, *Msx2* and *Prx2* are down-regulated (arrows in h, i, arrow in n, o). Other candidate marker genes, *Msx1* and *Prx1*, showed no remarkable changes.

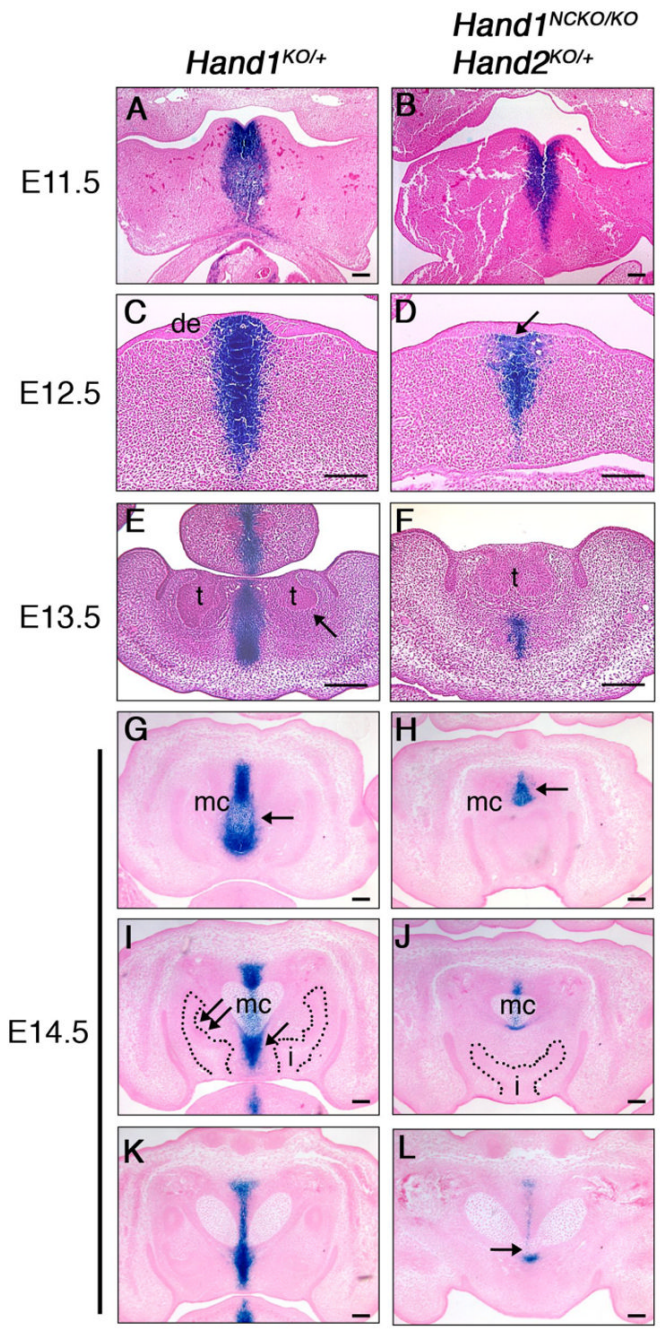

Figure 6. Development of *Hand1*-positive distal midline mesenchyme during embryogenesis

LacZ staining of *Hand1*$^{KO/+}$ (A, C, E, G, I, K) and *Hand1*$^{NCKO/KO}$;*Hand2*$^{KO/+}$ (B, D, F, H, J, L) embryos. Transverse sections (A–F) and coronal sections (G–L) are shown. **(A, B)** LacZ staining is observed in the distal tip of the mandibular arch in both wild-type and mutant embryos at E11.5. **(C, D)** At E12.5, two distinct thickenings of the dental epithelium (de) corresponding to the future incisors are observed in wild-type embryo (C), whereas one linear thickening of the epithelium was observed in the mutant (D, arrow). **(E, F)** In wild-type embryos, two well-developed incisor buds are observed. Strong lacZ staining was observed in the distal midline mesenchyme between the tooth buds and in the center of the tongue in wild-type embryo (E). Dental mesenchyme is negative for lacZ (E, arrow). In the mutant, lacZ-

positive mesenchyme is markedly reduced and tooth buds are fused (F). **(G–L)** Sections were taken in a distal (G, H) to proximal (K, L) direction in E14.5 embryos. In wild-type embryos, strong lacZ staining is detected in the distal symphysis of the Meckel's cartilage (G, arrow) and the inter-dental mesenchyme (I, arrow). Two cap-stage incisors are observed (i in I). Dental mesenchyme is negative for lacZ (I, double arrow). In the mutant, the distal symphysis is significantly reduced in size (H, arrow), and a single incisor is observed (i in J). The distal end of Meckel's cartilage is tapered and fused (arrow in L). t; tooth bud, i; incisor, mc; Meckel's cartilage. Bars indicate 100 μm.

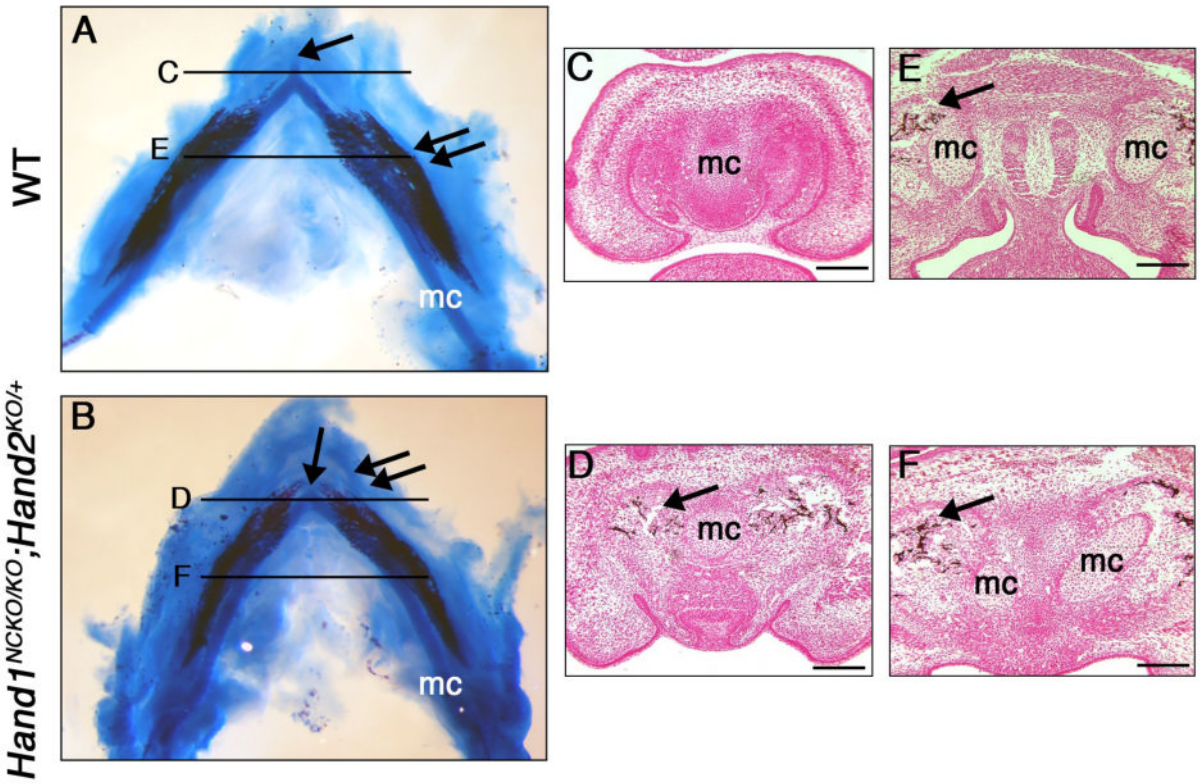

Figure 7. Premature mineralization of the mandible in *Hand1*$^{NCKO/KO}$; *Hand2*$^{KO/+}$ embryos

(A, B) Alcian blue and alizarin red staining of E14.5 wild-type (A) and *Hand1*$^{NCKO/KO}$;*Hand2*$^{KO/+}$ (B) embryos. In wild-type embryo (A), a well-developed distal symphysis of the Meckel's cartilage (arrow) and mineralization of the mandible (double arrow) is observed along the body of Meckel's cartilage. In the mutant (B), the distal symphysis is absent (arrow) and mineralization is accelerated at the distal portion of Meckel's cartilage (double arrows). **(C–F)** Coronal sections of the mandible from E14.5 wild-type (C, E) and mutant (D, F) embryos stained with Von Kossa. Levels are indicated in A and B. Mineralization is observed around the proximal portion of Meckel's cartilage in both wild-type and mutant embryos (arrow in E and F). In contrast, mineralization in the distal tip of the Meckel's cartilage is only observed in the mutant (arrow in D, compare C and D). Bars indicate 100 μm. mc; Meckel's cartilage.

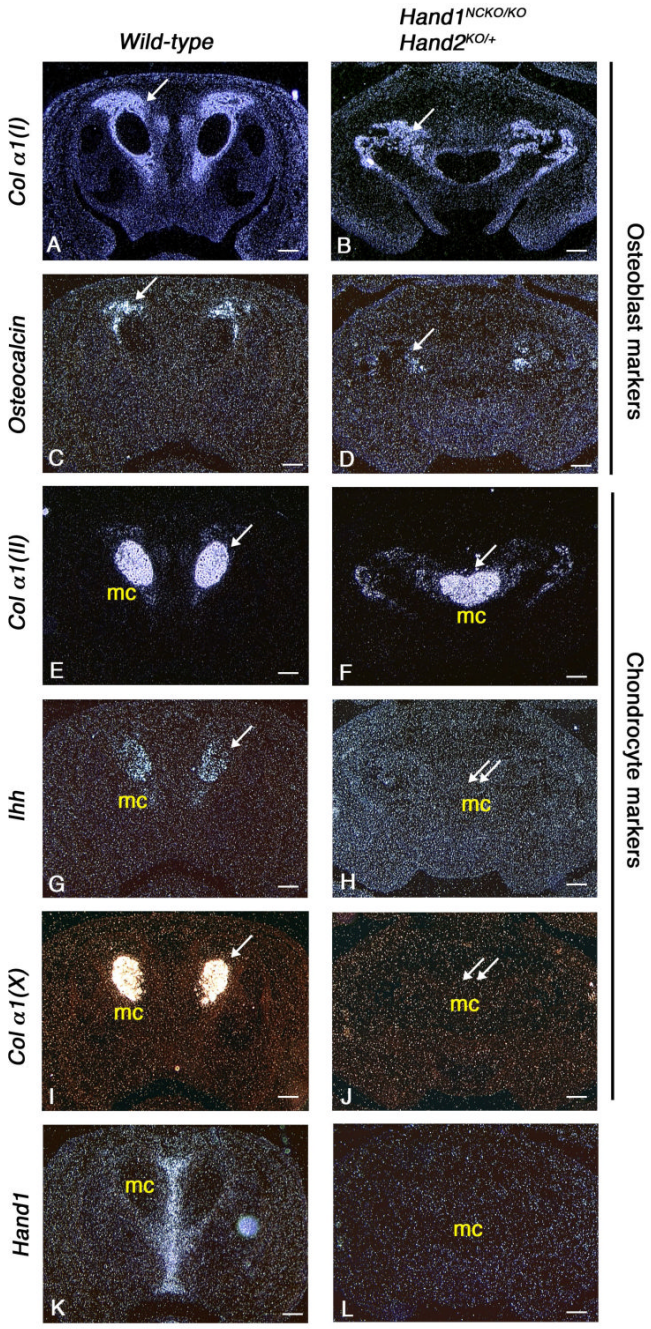

Figure 8. Expression of bone and cartilage differentiation markers in E14.5 wild-type and *Hand1NC*$^{KO/KO}$;*Hand2*$^{KO/+}$ embryos

Coronal sections of the mandible from wild-type (A, C, E, G, I, K) and mutant embryos (B, D, F, H, J, L) are hybridized with osteoblast differentiation markers (A–D) or chondrocyte differentiation markers (E–J). Membranous bone ossification takes place around Meckel's cartilage (arrows in A–D). While *collagen αI (I)* is expressed in both wild-type (A) and mutant (B) embryos, osteocalcin, a mature osteoblast marker, is down-regulated in the mutant (D). Note that *Ihh* and *collagen α1 (X)* expressed in the wild-type Meckel's cartilage (arrows in G, I) are absent in the mutant embryos (double arrows in H, J). *Hand1* expression performed as a control is absent in the mutant embryo (K, L). Bars indicate 100 μm.

Table 1

Summary of mandible staining of *Hand* mutants at P1

Genotype	N	Hypoplastic mandible	Fused mandible	Single lower incisor
Hand1$^{KO/+}$	10	0	0	0
Hand1$^{NCKO/KO}$ 1)	14	0	0	0
Hand1$^{KO/+}$; *Hand2*$^{KO/+}$	11	0	0	0
Hand1^{NCKO}; *Hand2*$^{KO/+}$	8	8/8 (mild)	8/8	8/8
Hand1^{NCKO}; *Hand2*$^{BA/+}$	8	1/8	1/8	0/8
Hand2$^{BA/BA}$	9	9/9 (severe 2))	0/9	0/9
Hand1^{NCKO}; *Hand2*$^{BA/BA}$	8	8/8 (severe)	7/8	5/8

1) This genotype includes Wnt1::Cre (+); *Hand1*$^{loxP/lacZ}$ and Wnt1::Cre (+); *Hand1*$^{loxP/loxP}$

2) Severe mandibular defects include truncation and absence of the angular process.